



B-KUL-H05U3: INTEGRATED PROJECT IN ENERGY

Design of a household PV & battery systems

Authors :

Lucas BOSSAERT (r0798521)

Victor EECKHOUT (r0778787)

Wout JORIS (r0786961)

Jesse KAMERLING (r0803453)

1 Introduction

2 Data Analysis for Solar Energy Optimization

2.1 Input data

The analysis of PV and battery systems across the various considered scenarios relies on two pivotal datasets, critical for the design and optimization of PV and battery storage solutions in residential contexts.

First, solar irradiance data is gathered using both unshaded and shaded pyranometers to accurately measure Global Horizontal Irradiance (GHI) and Diffuse Horizontal Irradiance (DHI), respectively. Additionally, this dataset incorporates temperature readings for PV panels situated on diverse roof types. Captured minutely throughout the entirety of 2018 by a meteorological measurement system at EnergyVille in Genk (50.99461°N, 5.53972°E), this dataset provides a detailed overview of the potential solar energy available for conversion to assess the performance of PV systems.

Second, the household load data reflects the electrical demand patterns (in kW) of Flemish households, with measurements taken every fifteen minutes, paralleling the solar data's timeframe. Derived from real-world consumption statistics, this dataset offers detailed insights into residential energy usage, crucial for tailoring PV and battery systems to meet specific household energy needs. Collectively, these datasets form the empirical bedrock of our study, enabling a detailed exploration of how solar energy potential, household energy consumption, and the efficiency of integrated PV and battery storage systems interact within a residential framework.

2.2 Data processing

VICTOR

2.3 Solar panel irradiance calculations

To calculate the power and energy flows within the system, the processed solar data is utilized to determine the effective irradiance on the solar panels, oriented in the considered directions and positioned at particular tilt angles. The total effective irradiance on a panel typically encompasses a direct, diffuse, and reflective component [1]. Nonetheless, due to the lack of data on and the negligible contribution of the reflective component for monofacial PV modules, this term is omitted from this analysis. Consequently, the global horizontal irradiance (GHI), representing the total amount of radiation received by a surface horizontal to the ground, comprises both the diffuse and direct irradiance components as shown in Equation 1 [2].

$$GHI = DHI + DNI \cdot \cos(\theta_z) \quad (1)$$

The term Diffuse Horizontal Irradiance (DHI) refers to the component of solar radiation that reaches the Earth's surface after being scattered or reflected by the atmosphere. On the other hand, Direct Normal Irradiance (DNI) denotes the portion of solar radiation that travels directly from the sun to the Earth without being scattered or absorbed by atmospheric elements. To calculate its contribution to solar power on a surface perpendicular to the ground, DNI must be adjusted for the solar zenith angle. The solar zenith angle measures the angle between the direction of direct sunlight and the vertical direction directly above a specific location on the Earth's surface. When the sun is directly overhead, the solar zenith angle is 0°, indicating that the sunlight is striking the surface perpendicularly.

Upon analyzing the solar dataset, it is observed that there are instances where the Global Horizontal Irradiance (GHI) is recorded as being lower than the Diffuse Horizontal Irradiance (DHI), a scenario that theoretically contradicts the principles outlined in Equation 1. These discrepancies predominantly arise under conditions of low GHI, typically during nighttime or overcast weather, suggesting a minimal absolute error magnitude. Such anomalies are most plausibly attributed to inaccuracies in the meteorological instrumentation or exceptional atmospheric conditions that lead to diffuse irradiance unaccounted for by the unshaded pyranometer, such as moonlight or artificial light pollution from surrounding activities. When encountering these inconsistencies, Direct Normal Irradiance (DNI) is consequently adjusted to zero for the purposes of subsequent analyses and computations.

Typically, PV panels are not installed horizontally but are instead tilted at specific angles relative to the ground to optimize power generation, aiming to better match the general demand curve they are intended to supply. On gable roofs, the tilt angle of the PV panels typically mirrors the roof's pitch, offering a predetermined inclination. Conversely, flat roofs allow for a higher degree of flexibility in choosing the panels' tilt angle, which will be further optimized in this section. Given the chosen tilt and orientation, the Global Tilted Irradiance, forming the base value for further module power calculations, is derived from a modified version of Equation 1. This adaptation, outlined in Equation 2, incorporates the effects of tilt and orientation through a specific incidence angle (θ) which represents the angle of direct sunlight relative to the panel surface's normal.

$$GTI = DHI + DNI \cdot \cos(\theta) \quad (2)$$

This incidence angle is dependent of four geometric angles: the tilt angle of the PV module (β), the module's orientation relative to the north (γ), the solar zenith angle (θ_z) and the solar azimuth angle (γ_s) as displayed in Figure 1. The initial two angles are determined by the module's orientation (Southern or East-West) and tilt, which is a degree of freedom in flat-roof installations that will need to be optimized. To ensure alignment with the irradiance data's minute-by-minute resolution, the solar angles for the specified location in Genk are computed using the PyEphem library. PyEphem is an astronomical library dedicated to executing high-precision calculations of celestial bodies' positions, including the sun [3].

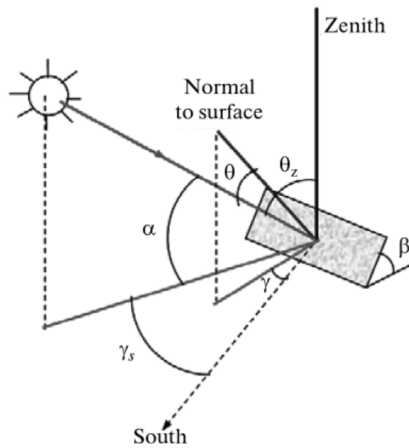


Figure 1: Angles in Solar Power calculations [4]

The cosine of the incident angle θ can be calculated using the dot product between the vector parallel to the direction of the DNI and the vector normal to the surface of the PV module. The formula for the dot product is given by Equation 3.

$$\mathbf{A} \cdot \mathbf{B} = |\mathbf{A}| |\mathbf{B}| \cos \theta \quad (3)$$

However, when considering unit vectors, the magnitudes $|\mathbf{A}|$ and $|\mathbf{B}|$ are both equal to 1. Consequently, the formula simplifies to Equation 4, with the DNI vector and the vector normal to the surface of the PV module serving as these unit vectors.

$$\cos(\theta) = \vec{r}_{\text{DNI}} \cdot \vec{r}_{\text{PV normal}} \quad (4)$$

The unit vectors are defined in a Cartesian coordinate system with the x-axis aligning with the east direction, the y-axis with the north, and the z-axis pointing towards the zenith. Since the solar azimuth angle is measured from the south in [4], contrary to the conventional measurement from the north, a 180° adjustment must be applied using trigonometry to derive the unit vector parallel to the direction of the DNI in Equation 5.

$$\vec{r}_{\text{DNI}} = \begin{bmatrix} \sin(\theta_z) \cdot (-\sin(\gamma_s)) \\ \sin(\theta_z) \cdot (-\cos(\gamma_s)) \\ \cos(\theta_z) \end{bmatrix} \quad (5) \quad \vec{r}_{\text{PV normal}} = \begin{bmatrix} \sin(\beta) \cdot \sin(\gamma) \\ \sin(\beta) \cdot \cos(\gamma) \\ \cos(\beta) \end{bmatrix} \quad (6)$$

The second unit vector, which represents the normal to the PV module, is defined by Equation 6. The tilt angle β is variable; however, it must be identical for both the east and west directions when an East-West orientation is assumed. For a PV module oriented towards the east, south, or west, the azimuth angle of the module's orientation γ is set to 90° , 180° , and 270° , respectively.

The Global Tilted Irradiance, as defined in Equation 2, can now be calculated using all the previously described parameters for the various orientations. It has been observed that on overcast days, the difference in irradiance profiles among the orientations, which is displayed in Figure 2 is relatively small. This is primarily due to the dominance of the diffuse component in Equation 2. However, on sunny days, a distinct difference in irradiance profiles is evident, as illustrated in Figure 3, for a tilt angle of 10 degrees for East-West oriented modules and angle of 40 degrees for South-oriented modules. Notably, the East-facing panel receives its peak irradiance in the morning, the South-facing panel around noon, and the West-facing panel in the afternoon. This sequence logically follows the sun's path across the sky. Additionally, the effect of diffuse irradiance becomes noticeable as well on days with a clear sky during periods without direct sunlight striking the PV module, such as close to sunrise and sunset, when the irradiance profiles for the different orientations will briefly converge.

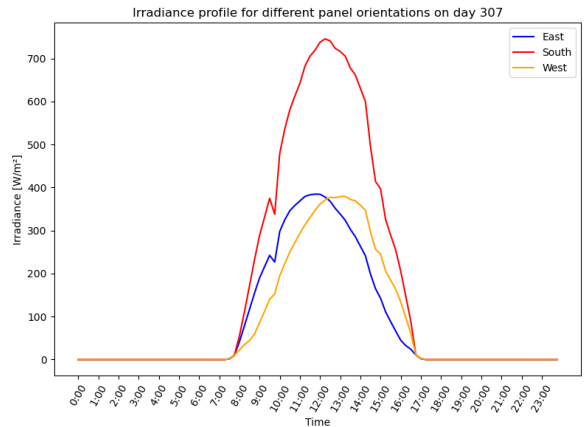
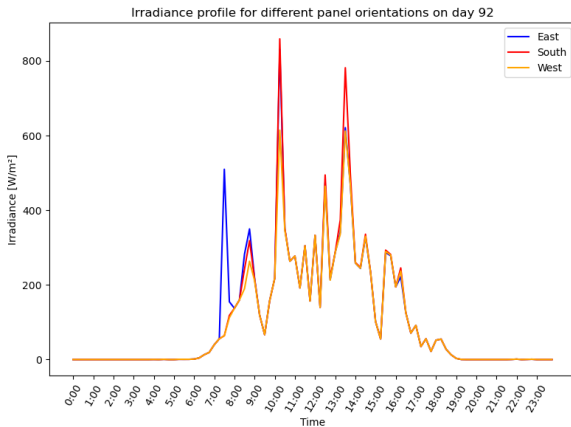


Figure 2: Irradiance day profile with overcast weather Figure 3: Irradiance day profile with clear sky

As previously discussed, the tilt angle represents a significant degree of freedom during the setup process for PV modules on flat roofs. The primary objective across the various cases is

to maximize the total solar energy yield of the PV modules. To achieve this, an optimization analysis was conducted, focusing on the total solar energy incident on the PV panels for both the East-West and Southern orientations. The analysis involved iterating over the Global Tilted Irradiance (GTI) integrated across the entire dataset for a year, over a range of tilt angles from 0 to 90 degrees. The resulting plot, shown in Figure 4, illustrates that for the Southern orientation, it is advantageous to position the PV modules at a specific angle. An optimal tilt of 40 degrees was identified at the Energyville facility based on the provided data. When these findings are benchmarked to existing data from Belgium found in the literature [5][6], they align with the outcomes of previous analyses ranging from 35 to 43 degrees for the region.

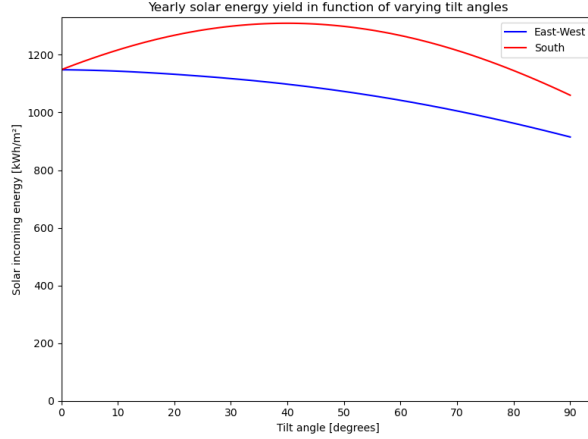


Figure 4: Yearly solar energy yield in function of varying tilt angles

For the East-West orientation, the analysis yielded a quadratic decreasing function, pinpointing the optimal configuration for PV modules as being completely horizontal. This finding, however, emerged from considering only the total incident solar energy yield as the optimization parameter. It is crucial to recognize that other factors also play pivotal roles in determining the ideal setup for PV modules. One compelling reason to deviate from the conventional Southern orientation is to better align power generation with daily load consumption patterns. Angling the modules can broaden the distribution of incident solar energy throughout the day, albeit at the expense of peak power and the aggregate solar energy incident on the modules. Additionally, installing the modules at an angle can mitigate the accumulation of dirt and dust and allow for the installation of more modules within a given surface area due to reduced space requirements. Consequently, the paper continues with a tilt angle of 10 degrees for East-West oriented panels, aligning with market standards such as the 12.5 degrees specified by certain sources, including [7]. This angle strikes a balance between maximizing energy yield and aligning energy production with consumption patterns, while also considering practical aspects such as maintenance and space utilization.

3 System description and Component selection

3.1 System overview

A variety of configurations are available for photovoltaic (PV) systems, dependent upon the objectives of the installation and specified boundary conditions. Within the scope of this project, solely grid-connected systems are investigated, both with and without a battery storage system. A disconnected, or off-grid system, is excluded from the analysis. This stems from the fact that these are generally less favourable in comparison to grid-connected systems, if a sufficiently developed grid is available. This is due to the fact that off-grid systems possess finite storage capabilities and lack the capability to draw surplus electricity from, or supply electricity to, the

grid. The two possible grid-connected configurations are illustrated by Figures 5 and 6 [8] [9].

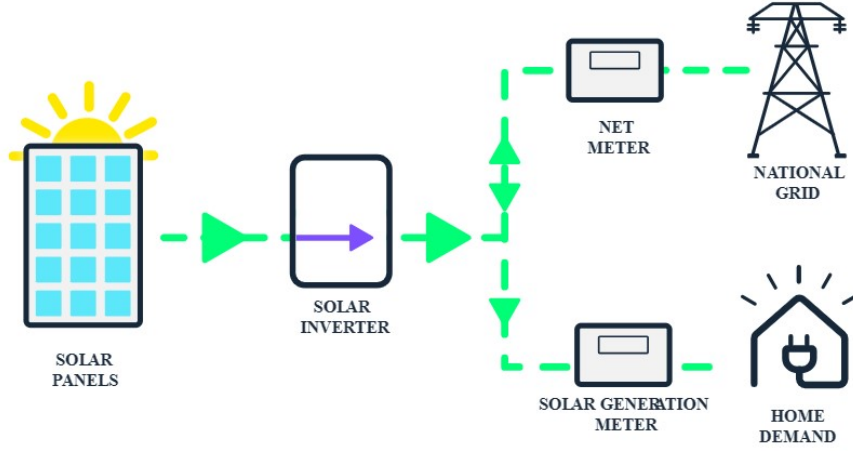


Figure 5: An on-grid solar system without batteries.

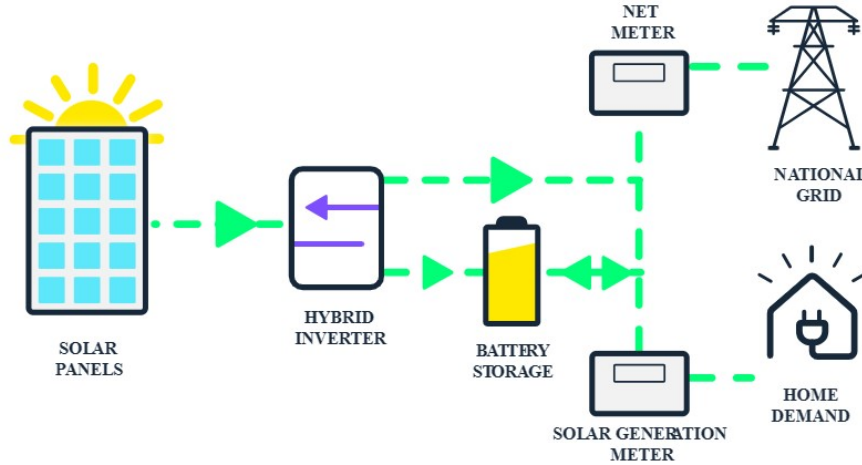


Figure 6: An on-grid solar system with batteries, also called a hybrid system.

In both installations, the solar panels, a certain type of inverter and the metering system constitute three key components, for which the inverter type is dependent on the system's topology. Moreover, a note has to be made regarding the metering systems shown on the figure. A solar and net meter is shown, however, both net and digital meters will be explained and analysed in detail. Furthermore, the second system utilises batteries for additional storage. In this configuration, a hybrid inverter is necessary. This inverter integrates the functionality of both a grid and battery converter, making it feasible to either store energy or convert it to alternating current. Each of these primary components will be discussed separately in following subsections. Other components such as a wiring, fuses and disconnection switches will be discussed together [9] [10].

Subsequently, the model will need to optimise the installation and thus the combination of components. Ideally, this would be done over the entire collection of market available components suitable for the installation. However, due to practical considerations, a limited amount of well-chosen options for each component are considered here. Following sections discuss these options

for the different components respectfully. Finally, Electrical Vehicles (EVs) will be discussed since these can have a significant impact on the demand profile.

3.2 Different components

This subsection provides a summary of the chosen components incorporated into the optimisation model. The diversity of these components will reveal which manufacturers produce the most efficient parts and the optimal photovoltaic (PV) settings for their use.

3.2.1 Solar panels

For the solar panels, three of the market leading manufacturers are taken into consideration, being Canadian Solar, RECOM and Trina Solar. For each of these suppliers, two different types of panels are chosen which vary in conversion efficiency, max generated power, dimensions, price etc. This causes to have a market sample with substantial variation. All these datasheets are added in appendix ??.

3.2.2 (Hybrid) Inverters

As said before, the choice of inverter is based on the configuration that is used. For the configuration in Figure 5, two different manufactures are chosen, namely SMA and Victron Energy. Since both manufacturers are well known, the hybrid inverters are chosen to be similar but with different operational characteristics. See appendix ??¹ for more specifications.

3.2.3 Batteries

To ensure optimal compatibility with the hybrid inverters, the selected batteries are also from SMA and Victron Energy. These batteries have a cell technology called lithium iron phosphate, with energy capacities ranging from 0,64kWh to 16,4kWh. To achieve such capacities, the batteries are designed to be stackable. Appendix ?? gives more information regarding the characteristics.

3.2.4 Digital/net metering

When faced with the decision between an analog and a digital meter, several key factors come into play, each depending on the specific needs and preferences of the user. In terms of tariffs, the analog meter adopts a straightforward approach; it records the annual net consumption, applying a uniform capacity price per kWh to the consumer's usage. The digital meter, on the other hand, offers a more frequent measurement by recording usage every fifteen minutes, facilitating the implementation of complex tariff structures. Each month, the highest usage peak is identified, and the consumer is billed a capacity tariff based on the average of these monthly peaks.

3.2.5 Other necessities

3.3 Electric vehicle

As said before, EVs can have a significant impact on the demand profile, which can affect the optimal number of solar panels or the advantage of incorporating batteries in the PV system. This analysis evaluates the impacts on the photovoltaic system using two distinct vehicles: a Tesla Model S and a Citroën Ami. Given the variance in their characteristics, including price,

¹Victron Energy has hybrid inverters with one or two trackers, which determine the number of PV arrays that can be connected.

range, and capacity, it's anticipated that the effects they have on the PV system will differ. This comparative approach allows us to understand how different vehicle specifications might influence the PV system's performance and efficiency.

3.4 Extensions

4 Power flow analysis

4.1 Theoretical analysis

The primary aim of the power flow analysis is to determine all power flows present in the system, from solar power input to consumption. This analysis is conducted for two distinct scenarios, namely without or with a battery system in place. In each case, the power flows are graphically presented in figures 7 and 8. Following subsections will step by step discuss the calculation of these flows and the efficiencies present [9].

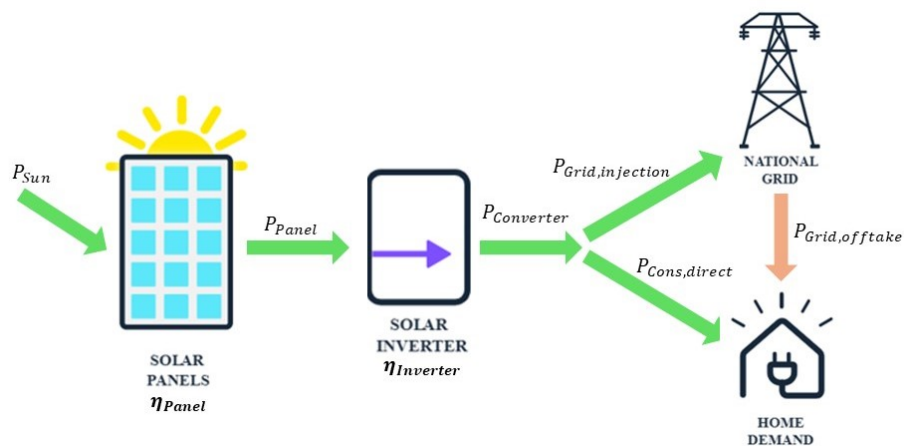


Figure 7: The power flows in a system without batteries [9].

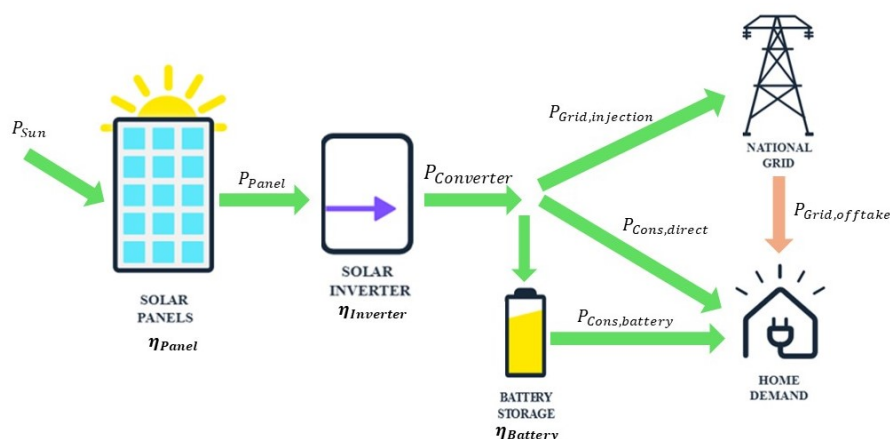


Figure 8: The power flows in a system with batteries [9].

Table 1: Different factors contributing to the total solar panel efficiency η_{Panel} [11].

	Value	Explanation
η_{Cell}	20.46-23%	The cell efficiency is given by the manufacturer and can thus be found in the respective datasheets.
η_{Shade}	100%	Assumption is made that not shade is present due to neighbouring buildings or trees.
$\eta_{Obstruct}$	100%	Assumption is made that no dirt or other materials are present on the panels. To achieve (near) this value, regular maintenance is necessary.
η_{Temp}	Formula 10	The influence of the temperature is a linear decreasing function of the panel temperature.
η_{Degrad}	Formula 11	The panel degradation can be approximated by a linear decreasing function of the time.

4.1.1 Power PV panels

Section two delineates the computation of the Global Total Irradiance (GTI) on a inclined solar panel orientated towards a specific azimuth angle. Subsequently, to compute the total solar power P_{Sun} received, it is necessary to multiply this value by the quantity of solar panels n and the area A of each panel, as described by equation 7. The power supplied by the panels to the inverter P_{Panel} is determined by equation 8.

$$P_{Sun} = GTI \cdot n \cdot A \quad (7)$$

$$P_{Panel} = P_{Sun} \cdot \eta_{Panel} \quad (8)$$

The panel efficiency η_{Panel} is influenced by various factors, such as the cell efficiency, shading, obstructions, temperature, degradation etc. This is demonstrated in equation 9, for which each of these efficiencies are exemplified by table 1. However, the temperature and degradation dependencies will be further elucidated in the next paragraph. Furthermore, the assumption is made that each panel receives identical uniform irradiation at each time instance. Cloud coverage differences between panels is therefore neglected, since this influence is already present in the solar measurement data, as described by section two [11].

$$\eta_{Panel} = \eta_{Cell} \cdot \eta_{Shade} \cdot \eta_{Obstruct} \cdot \eta_{Temp} \cdot \eta_{Degrad} \quad (9)$$

As said, further elaboration is necessary regarding both the temperature and degradation dependencies. Firstly, concerning the temperature-related efficiency, this can be approximated using equation 9 as was done by Evans [?]. In this equation, T_{ref} denotes the reference temperature, typically set at 25°C (or 298.15 K), T_c represents the cell temperature and β_{ref} signifies the temperature coefficient. The latter parameter is provided by the manufacturer and can be found in the appended data sheets [?].

$$\eta_{temp} = 1 - \beta_{ref} \cdot (T_c - T_{ref}) \quad (10)$$

Secondly, regarding the influence of degradation, it is recognised that all panels experience a decrease in efficiency over time. The rate of efficiency decline depends on various factors which. However, an initial approximation can be made which states an average efficiency reduction of around 0.5% per year. Mathmatically, this degradation factor η_{Degrad} per day t is given by equation 11. As visible, this factor remains proximal to unity and thus may be neglected in preliminary analysis [12].

$$\eta_{Degrad} = 1 - 0.005 \cdot \frac{t}{365} \quad (11)$$

4.1.2 Inverter power

the inverter

4.1.3 Case 1

In case one, the solar inverter is solely responsible for converting the power from DC to AC. This conversion occurs with a certain efficiency $\eta_{Converter}$ as shown by equation 12. The value for the converter efficiency is given in the data sheet of the supplier. If the supplied power from the panels exceeds the inverter capacity, this conversion will be limited to this power $P_{Converter,maximal}$ given in its respective data sheet.

$$P_{Converter} = \eta_{Converter} \cdot P_{Panel} \text{ if } P_{Converter} < P_{Converter,maximal} \quad (12)$$

Following the conversion process, the power is either directly consumed by the connected loads or injected in the grid. In instances where the power generated by the panels exceeds the total instantaneous load, the surplus is injected into the grid. Conversely, if the generated power is insufficient to meet the total demand, additional power is drawn from the grid. These relations are shown by equations 13 and 14.

$$P_{Grid,injection} = P_{Converter} - P_{Cons,direct} \text{ if } P_{Converter} > P_{Load} \quad (13)$$

$$P_{Grid,offtake} = P_{Load} - P_{Converter} \text{ if } P_{Converter} < P_{Load} \quad (14)$$

4.1.4 Case 2

Case two is characterised by the presence of a Hybrid inverter that is capable of supplying AC and DC power to both consumption side and the battery system respectfully. This component is generally capable of managing the power supply to optimise consumption and charging behaviour to minimise the electricity cost. Therefore, as visible in figure 14, The power distribution after the inverter works differently in comparison to case one. However, as an approximation, formula 12 holds for the hybrid inverter as well, with its conversion efficiency given in the data sheets.

The power is primarily supplied to meet the loads and thus inverted from DC to AC. To approximate the optimisation behaviour of the hybrid inverter, following assumptions are made. In instances where the power generated by the panels exceeds the total instantaneous load, the hybrid inverter will charge the batteries to store energy. If this for some reason is unavailable, or the battery is full, excess energy is injected into the grid. Conversely, if the generated power is insufficient to meet the total demand, additional power is either drawn from the battery and/or from the grid, giving preference to the battery system if this is available and sufficient. It could be that the power discharge rate of the battery is too small in comparison to the needed remaining load, in that case the grid offtake will come to assistance. The battery system itself has a round trip efficiency given in the datasheets. These relations are expressed by equations xxx-xxx.

For the Battery system (if this battery system is not full yet and sufficient capacity is available, otherwise it is limited to its available charge capacity, discharge capacity or available system capacity) following equations hold.

$$P_{Battery,charge} = P_{Inverter} - P_{cons,direct} \text{ if } P_{Inverter} < P_{Inverter,max} \text{ and } P_{Inverter} > P_{cons,direct} \quad (15)$$

$$P_{Battery,charge} = P_{Inverter,max} \text{ if } P_{Inverter} - P_{cons,direct} > P_{Inverter,max} \quad (16)$$

$$P_{Battery,discharge} = P_{load} - P_{cons,direct} \text{ if } P_{Battery,discharge} + P_{cons,direct} < P_{Load} \quad P_{Battery,discharge} = P_{discharge,max} \text{ if } P_{Battery,discharge} + P_{cons,direct} \geq P_{Load} \quad (17)$$

For the rest of the system:

$$P_{grid,injection} = P_{Inverter} - P_{Cons,direct} - P_{Battery,charge} \text{ if } P_{Battery,charge} + P_{Cons,direct} < P_{Inverter} \quad (18)$$

$$P_{grid,offtake} = P_{load} - P_{Cons,direct} - P_{Battery,discharge} \text{ if } P_{Battery,discharge} + P_{cons,direct} < P_{Inverter} \quad (19)$$

Algorithm 1 Power modeling sequence (battery case)

```

1: procedure POWER MODELING SEQUENCE( $P_{inverter}, P_{battery,charge,MAX}, P_{battery,discharge,MAX}, P_{load}, E_{battery}$ )
Ensure:  $E_{battery} = P_{battery,charge} \cdot \Delta t \leq E_{battery,max}$ 
2:   for all  $\Delta t$  do
3:     if  $P_{inverter} > P_{inverter,max}$  then
4:        $P_{inverter} \leftarrow P_{inverter,max}$  ▷ More generation, then nominal inverter power
5:     end if
6:     if  $P_{inverter} > P_{load}$  then
7:        $P_{direct\ consumption} \leftarrow P_{load}$  ▷ Consume
8:        $P_{excess} \leftarrow P_{inverter} - P_{load}$ 
9:       if  $E_{battery} < E_{battery,max}$  then ▷ Battery not full yet
10:         $P_{charge,MAX} \leftarrow \min(P_{battery,charge,MAX}, \frac{E_{battery,max} - E_{battery}}{\Delta t})$  ▷ Can't charge
        faster than max charging capacity
11:        if  $P_{excess} > P_{charge,MAX}$  then
12:           $P_{battery,charge} \leftarrow P_{charge,MAX}$ 
13:           $E_{battery} += P_{battery,charge} \cdot \Delta t$  ▷ Charge battery
14:           $P_{injection} \leftarrow P_{excess} - P_{battery,charge}$  ▷ inject excess
15:        else
16:           $P_{battery,charge} \leftarrow P_{excess}$ 
17:           $E_{battery} += P_{battery,charge} \cdot \Delta t$  ▷ Charge battery
18:           $P_{injection} \leftarrow 0$ 
19:        end if
20:      else
21:         $P_{injection} \leftarrow P_{excess}$  ▷ Inject when battery is full
22:      end if
23:    else ▷ load demand is greater then generation
24:       $P_{direct\ consumption} \leftarrow P_{inverter}$  ▷ Consume
25:       $P_{short} \leftarrow P_{load} - P_{inverter}$ 
26:      if  $E_{battery} > 0$  then ▷ Battery not empty yet
27:         $P_{discharge,MAX} \leftarrow \min(P_{battery,discharge,MAX}, \frac{E_{battery}}{\Delta t})$  ▷ Can't discharge faster
        than max discharging capacity
28:        if  $P_{short} > P_{discharge,MAX}$  then
29:           $P_{battery,discharge} \leftarrow P_{discharge,MAX}$ 
30:           $E_{battery} -= P_{battery,discharge} \cdot \Delta t$  ▷ Discharge battery
31:           $P_{takeoff} \leftarrow P_{short} - P_{battery,discharge}$  ▷ take off shortage
32:        else
33:           $P_{battery,discharge} \leftarrow P_{short}$ 
34:           $E_{battery} -= P_{battery,discharge} \cdot \Delta t$  ▷ Discharge battery
35:           $P_{takeoff} \leftarrow 0$ 
36:        end if
37:      else
38:         $P_{takeoff} \leftarrow P_{short}$  ▷ takeoff when battery is empty
39:      end if
40:    end if
41:  end for
42: return  $P_{injection}, P_{takeoff}, P_{direct\ consumption}$ 
43: end procedure

```

References

- [1] M. H. Hakemzadeh, A. Ibrahim, K. Sopian, A. S. A. Hamid, and H. Jarimi, “Incorporating theoretical and practical approaches to assess the amount of sunlight captured by a tilted surface in a tropical climate,” *Heliyon*, vol. 9, no. 3, p. e14661, 2023.
- [2] A. VR, “Solar irradiance calculation guide,” 22/07/2022. Accessed: 2023-04-10.
- [3] R. B. Goldberg, “Pyephem: High-precision astronomy computations for python.” <https://github.com/brandon-rhodes/pyephem>, 2020. Accessed: 2024-04-10.
- [4] N. M and S. T., “Study on solar geometry with tracking of collector,” *Allerton Press*, vol. 51, pp. 274–282, 2015.
- [5] M. Z. Jacobson and V. Jadhav, “World estimates of pv optimal tilt angles and ratios of sunlight incident upon tilted and tracked pv panels relative to horizontal panels,” *Solar Energy*, vol. 169, pp. 55–66, 2018.
- [6] A. Robinson, “Solar pv potential in belgium by location,” 2024. Accessed: 2024-04-08.
- [7] Avasco Solar, “East-west oriented pv systems,” 2024. Accessed: 2024-04-08.
- [8] SolarSME, “Pros and cons of off-grid solar,” 04/03/2024.
- [9] Deegesolar, “The different types of solar pv systems,” 26/05/2022.
- [10] SMA, “Hybrid inverters,” 2024.
- [11] Kolkowska, M, “Factors affecting solar panel output,” 2023.
- [12] Simms, D, “Do solar panels lose efficiency over time?,” 2024.